International Journal of Heat and Mass Transfer 127 (2018) 1064–1076

Contents lists available at ScienceDirect

International Journal of Heat and Mass Transfer

journal homepage: www.elsevier.com/locate/ijhmt

Heat transfer enhancement for laminar flow in a tube using bidirectional conical strip inserts

Peng Liu, Nianben Zheng, Feng Shan, Zhichun Liu, Wei Liu *

School of Energy and Power Engineering, Huazhong University of Science and Technology, Wuhan 430074, China

ARTICLE INFO

Article history:
Received 9 October 2017
Received in revised form 3 July 2018
Accepted 25 July 2018

Keywords:
Bidirectional conical strip inserts
Multiple longitudinal swirling flows
Laminar tube flow
Heat transfer enhancement

ABSTRACT

In the present work, a novel tube insert (bidirectional conical strip inserts) is proposed, and the heat transfer performance and flow characteristics of this insert are studied numerically. Effects of three geometric parameters (numbers of bidirectional conical strip (n), central angle (α) and pitch ratio ($P^* = p/D$)) are also investigated. The results indicate that cold fluid in the core region and the hot fluid near the tube wall are rapidly exchanged as the fluid flows through the bidirectional conical strip, and multiple longitudinal swirling flows are formed downstream of the bidirectional conical strip. Therefore, the heat transfer (the Nusselt number) is significantly enhanced by 2.35–9.85 times compared to the smooth tube. Moreover, because of the cooperation between the forward and the reverse conical strips, the formation of the dead zone and eddy on the back of the conical strips is inhibited. Thus, the increase in flow resistance is smaller than many other published works, as the friction factor is enhanced to 2.37–21.18 times of the smooth tube. The overall heat transfer performance (*PEC* value) is located in range of 1.75–3.93. Both the Nusselt number and friction factor increase with the increasing numbers of bidirectional conical strip, central angle and the decreasing pitch ratio. However, the friction factor is more sensitive to geometric parameters, so the maximum overall heat transfer performance (PEC value) is obtained at moderate geometric parameters ($n = 3$, $\alpha = 40°$ and $P^* = 3$). In addition, Correlation formulas for Nusselt number and friction factor are derived.

1. Introduction

Heat exchange tubes are common units in various heat exchangers, which are widely applied in many industries such as power generation, waste heat recovery, chemical industry, etc. Heat transfer enhancement techniques for heat exchange tube have a great significance for energy saving and environmental protection. With the development for several decades, a variety of techniques for heat transfer enhancement in tube flow have been proposed and investigated.

In general, the passive methods are widely used because of their requiring no external power [1,2]. There are two common passive methods to enhance the convective heat transfer in tube flow. One is shaped tube or modification of tube wall, which focuses on the heat transfer augmentation in tube boundary layer, such as corrugated tube [3–6], ribbed tube [7,8], grooved tube [9,10], helically-finned tube [11], elliptical axis tubes [12], etc. The other is tube inserts, which enhances the heat transfer in the core flow and is widely researched because of its ease of manufacture and installation. Twisted tape, the most widely used tube insert, can induce turbulence and vortex motion (swirling flow) and consequently result in a higher heat transfer coefficient. Since Manglik and Bergles et al. [13,14] conducted experimental investigations on heat transfer and pressure drop in a tube fitted with twisted tape in laminar and turbulent flow regime, researchers all over the world have proposed and investigated various modifications of twisted tape [15]. Saha et al. [16] experimentally investigated the friction and heat transfer characteristics of laminar flow in a tube with regularly spaced twisted-tape inserts. They found that compared to the full-length twisted-tape, the friction factor for regularly spaced twisted-tape inserts was substantially decreased. Wongcharee et al. [17] studied the heat transfer and friction characteristics of laminar flow in tube fitted with alternate clockwise and counter-clockwise twisted-tapes. Guo et al. [18] proposed a center-cleared twisted-tape and numerically studied its heat transfer and friction factor characteristics in laminar flow regime. They found that the friction factors of center-cleared or centrally hollow narrow twisted tapes were obvious less than that of the traditional twisted tapes. Some cut or perforated twisted tapes have been

* Corresponding author.
E-mail addresses: peng_liu@hust.edu.cn (P. Liu), ben@hust.edu.cn (N. Zheng), shanfeng@hust.edu.cn (F. Shan), zcliu@hust.edu.cn (Z. Liu), w_liu@hust.edu.cn (W. Liu).

https://doi.org/10.1016/j.ijheatmasstransfer.2018.07.128
0017-9310/

Nomenclature

c_p	specific heat at constant pressure of water, J/kg·K
D	inner diameter of the tube, mm
D_1	distal diameter of the bidirectional conical strip, mm
d	proximal diameter of the bidirectional conical strip, mm
f	friction factor
f_0	friction factor of a smooth tube
h	heat transfer coefficient, W/m^2·K
L	the full length of tube, mm
Nu	Nusselt number
Nu_0	Nusselt number of a smooth tube
n	the number of bidirectional conical strip
P	pressure of water, Pa
p	the pitch of bidirectional conical strip, mm
P^*	pitch ratio
PEC	comprehensive heat transfer performance coefficient
q	heat transfer rate per unit area, W/m^2
R	inner radius of the tube, mm
r	the distance between the fluid particle and the center of the tube, mm
Re	Reynolds number
T	temperature of water, K
T_c	temperature at the center position of inlet Cross-section, K
u_i	the velocity component in the three-dimensional space, m/s
T_w	temperature on the tube wall, K
T_m	fluid bulk temperature inside tube, K
u	flow velocity, m/s
u_c	velocity at the center position of inlet Cross-section, m/s

Greek symbols

α	central angle of single bidirectional conical strip, °
δ	thickness of the bidirectional conical strip, mm
θ	the attack angle of bidirectional conical strip, °
λ	thermal conductivity of water, W/m·K
μ	dynamic viscosity of water, kg/m·s
ρ	density of water, kg/m^3

proposed and reported to improve the overall heat transfer performance in tube flow, such as V-cut twisted tape insert [19], square-cut twisted tape [20], multiple square perforated twisted tape [21] and so on. In addition to the twisted tape inserts, researchers have proposed and reported a variety of tube inserts. Ozceyhan et al. [22] numerically studied the heat transfer enhancement in tube flow using circular cross sectional rings. Tu et al. [23] found the tube with small pipe inserts could obtain a better thermal performance due to the pipe inserts pushing the maximum velocity water to the wall side. Louvered strip inserts fitted in circular tube

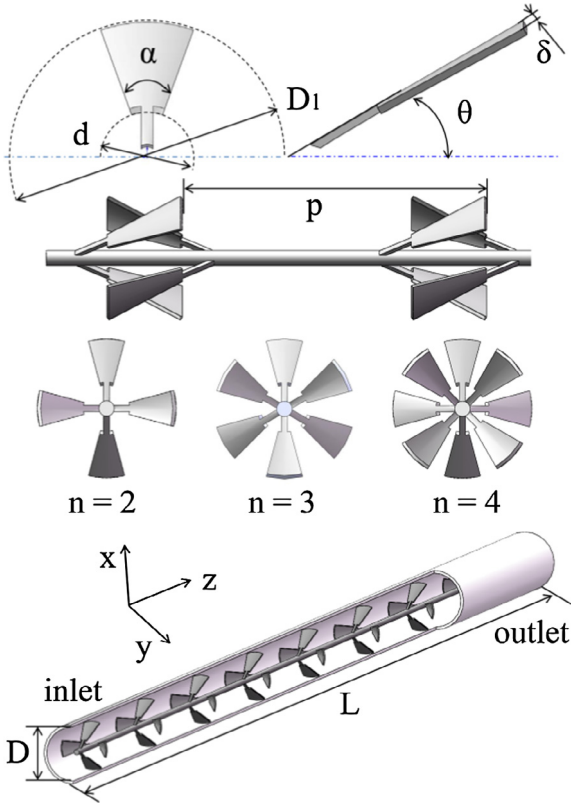

Fig. 1. Geometry model of bidirectional conical strip inserts, and the schematic diagram of a tube with bidirectional conical strip inserts.

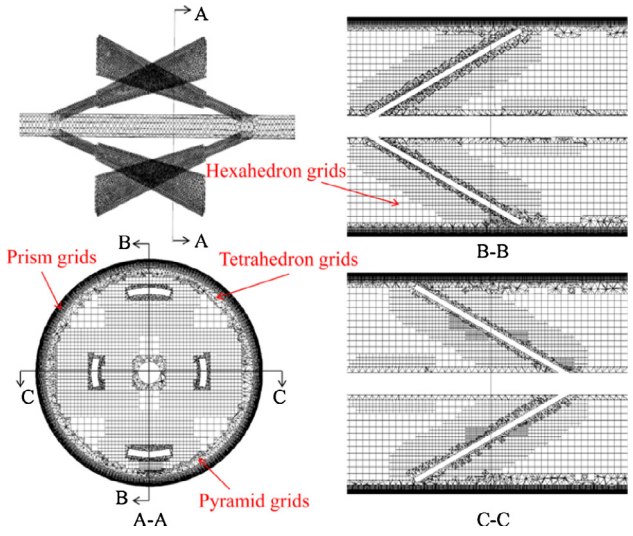

Fig. 2. Grids generated for computation domain.

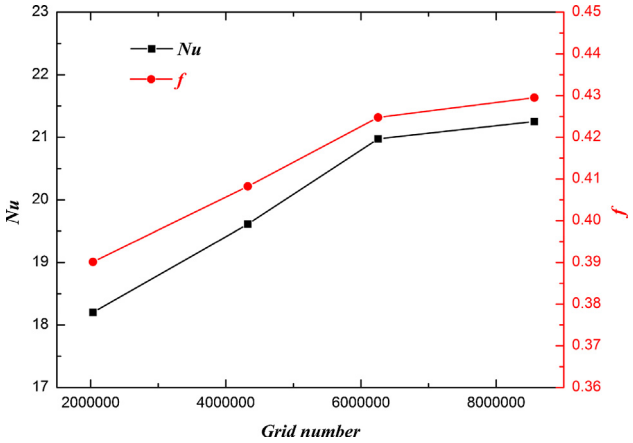

Fig. 3. Nusselt number and friction factor obtained by different grid systems for bidirectional conical strip insert with $n = 2$, $P^* = 2$ and $\alpha = 30°$, at $Re = 900$.

were numerically studied by Fan et al. [24] to characterize the thermo-hydraulic performance in turbulent flow regime. Zhang et al. [25] performed field synergy principle and entransy dissipation extremum principle analysis to investigate the mechanism of the heat transfer enhancement of a tube fitted with double spiral spring. Deshmukh et al. [26] carried out an experimentally study on heat transfer enhancement in tubes using curved delta wing vortex generator inserts in laminar flow regime. A twisted conical strip insert was proposed by Pourramezan et al. [27] for thermal augmentation of turbulent flow in a circular tube. Zhu et al. [28] reported a wavy-tape insert prototype for heat transfer enhancement in laminar flow regime in a tube. Jasiński [29] proposed a ball turbulators and conducted a study on its thermo-hydraulic characteristics in a circular tube flow. Nanan et al. [30] experimentally and numerically studied the turbulent forced convective heat transfer behaviors in a tube inserted with baffle turbulators and compared the thermo-hydraulic characteristics of several different structures of baffle. Z. Cao et al. [31,32] proposed modulated heat transfer tubes with consecutive conical-mesh inserts and mesh cylinder inserts, which can modulate flow and temperature fields and increase velocity gradient near tube wall and hence enhance heat transfer in tube.

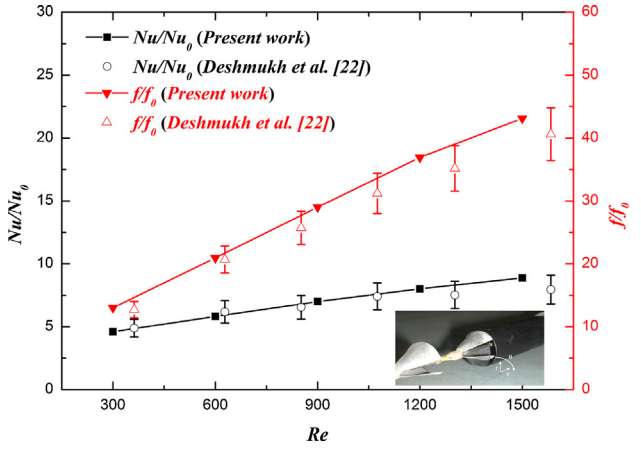

Fig. 4. Validation results for the Nusselt number ratio and friction factor ratio of a tube with curved delta wing vortex generator inserts.

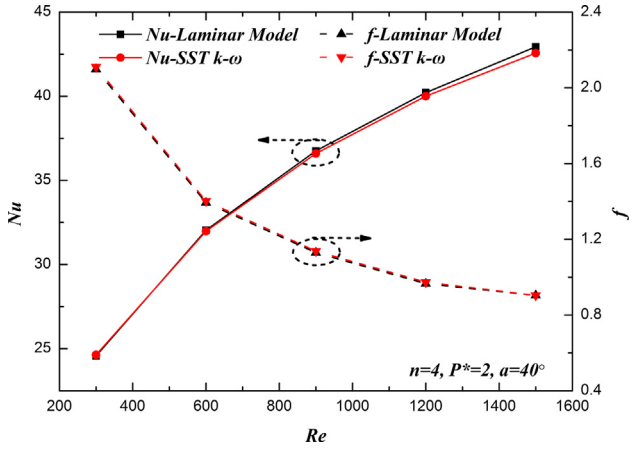

Fig. 5. Comparisons of Nusselt number and friction factor between the laminar model and SST k-ω turbulence model.

However, the augmentation of heat transfer in tube flow is always accompanied by a significant increase in flow resistance, which causes increase of pumping power. Hence, how to achieve a high heat transfer rate without much increase in the pressure drop becomes the goal and direction for heat transfer enhancement research. Motivated by this target, some researchers have carried out several heat transfer optimization studies [33–36] in tube flow based on the second law of thermodynamics. All the theoretical results show that a flow pattern with multiple longitudinal swirl flows can obtain a high overall heat transfer performance. To achieve the multiple longitudinal swirl flow structure in tube flow, we proposed central slant rods inserts in our previous work [37]. We found that the tube with central slant rods obtained an effective enhancement in heat transfer with little increase in the pressure drop. In addition, we found a higher overall heat transfer performance could be obtained if the vortex strength can be further intensified. Deshmukh et al. [26] reported that conical strip could form strong vortexes in tube flow. However, at the same time, dead zone and eddy, which would significantly increase the flow resistance in tube, were induced on the back of the conical strips. Based on the analysis above, we have proposed the bidirectional conical strip inserts, as shown in Fig. 1. The cooperation between the forward and the reverse conical strips may inhibit the formation of the dead zone and the eddy on the back of the conical strips. In addition, a parameter study was also conducted to optimize the geometric configurations of the inserts for practical applications.

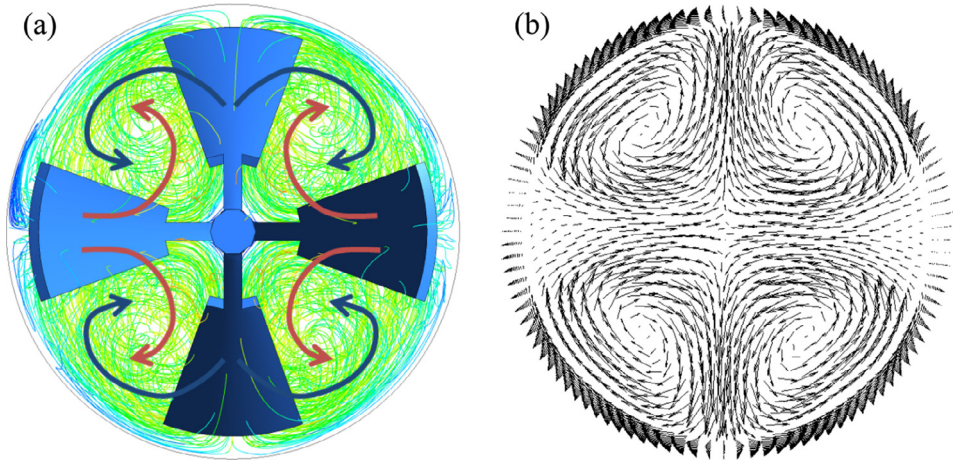

Fig. 6. Flow structures in the tube with bidirectional conical strip at Re = 900, n = 2, P^* = 2 and α = 40°, (a) streamline; (b) tangential velocity vectors.

2. Physical model description

The bidirectional conical strip insert is made by attaching the conical strips to a central rod in forward and reverse directions, which are in interval and symmetric distribution, as shown in Fig. 1. The conical strips are carved up from a conical ring with a certain central angle α and its thickness (δ) is 0.5 mm. The diameters of the big end (D_1) and the small end (d) of the conical strip are 18 and 6 mm, respectively. The diameter of the central rod is 2 mm, and the conical strips are attached to the central rod at a 30° slant angle ($\theta = 30°$). The heat exchanger tube in this work has a full length (L) of 500 mm and an inner diameter (D) of 20 mm. The effects of three geometric parameters on heat transfer and flow resistance are investigated in the present work. They include three central angles ($\alpha = 20°$, 30°, 40°), three strip pitch ratios, which are defined as the ratio of strip pitch to the tube inner diameter ($P^* = p/D = 2, 3, 4$), and three numbers of bidirectional conical strip ($n = 2, 3, 4$). Each bidirectional conical strip includes one pair of forward and reverse conical strips.

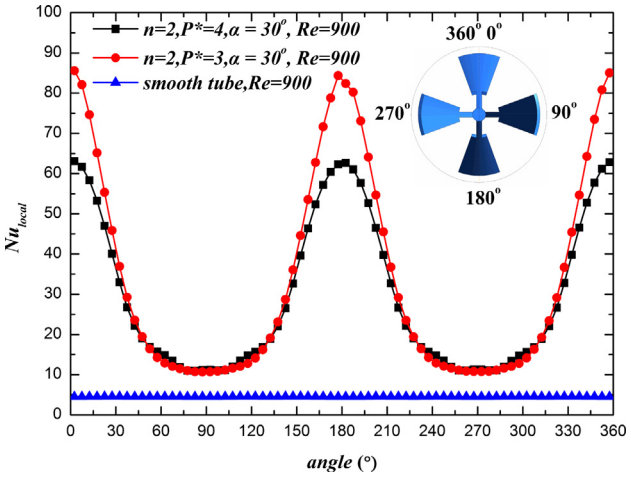

Fig. 7. Circumferential local Nusselt number along the tube wall perimeter.

3. Numerical model description

3.1. Governing equations and boundary conditions

The range of Reynolds number studied in this paper is from 300 to 1500, which is in laminar flow regime for flow in a smooth circular tube. The computation domain in this work is assumed to be three-dimensional, laminar and steady. Water is selected as the working fluid. The following assumptions are made to obtain the mathematic model: (1) the physical properties of fluid are constant; (2) The fluid is Newtonian, incompressible, isotropic and continuous; (3) The deformation and vibration of insert are neglected; (4) the influences of viscous heating, thermal radiation and gravity are negligible. The governing equations of continuity, momentum and energy for time-averaged fluid flow are listed as follows:

$$\text{Continuity equation}: \frac{\partial u_i}{\partial x_i} = 0 \quad (i = 1{-}3) \tag{1}$$

$$\text{Momentum equation}: \rho u_i \frac{\partial u_i}{\partial x_i} = -\frac{\partial p}{\partial x_i} + \frac{\partial}{\partial x_i}\left(\mu \frac{\partial u_i}{\partial x_i}\right) \quad (i = 1{-}3) \tag{2}$$

$$\text{Energy equation}: \rho c_p (u_i \frac{\partial T}{\partial x_i}) = \lambda \left(\frac{\partial^2 T}{\partial x_i^2}\right) \quad (i = 1{-}3) \tag{3}$$

where λ and ρ is heat conductivity coefficient and density of fluid respectively.

A constant heat flux condition of 2000 W/m^2 is imposed on the tube wall. The fully developed profiles of velocity and temperature, which are defined as Eqs. (4) and (5), are employed at the inlet to

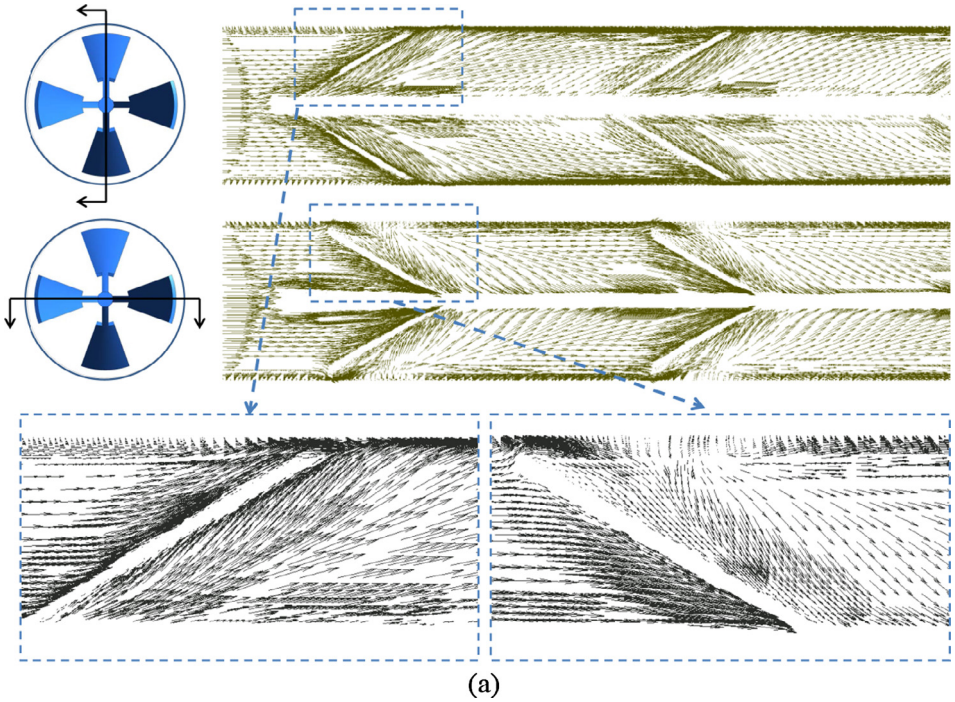

Fig. 8. Results of tube with bidirectional conical strip insert at $Re = 900$, $n = 2$, $P^* = 2$ and $\alpha = 40°$: (a) tangential velocity vectors of axial sections, (b) temperature contours of axial sections, (c) temperature contours of cross sections.

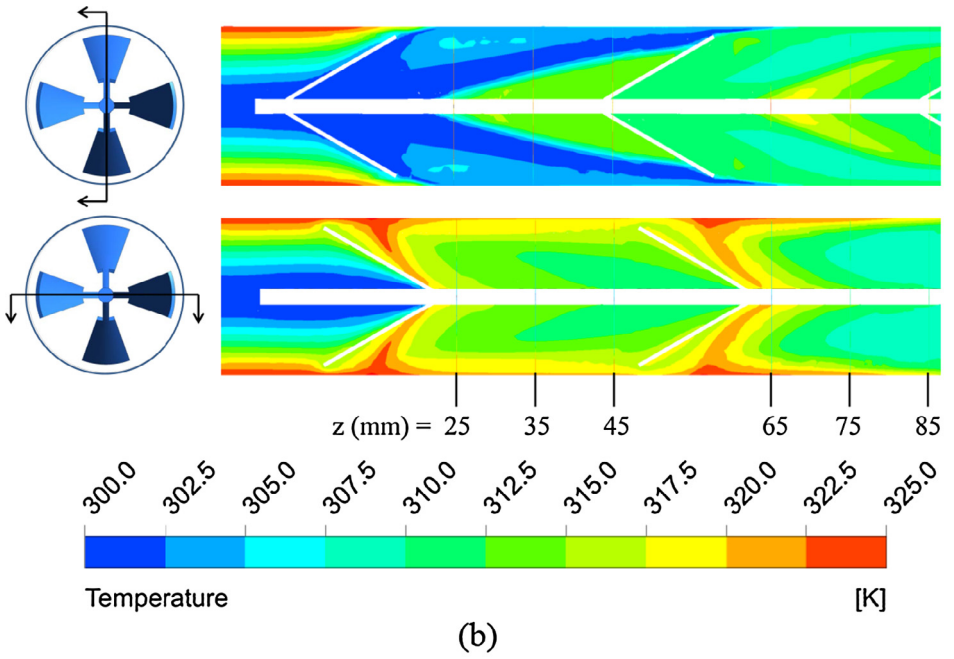

(b)

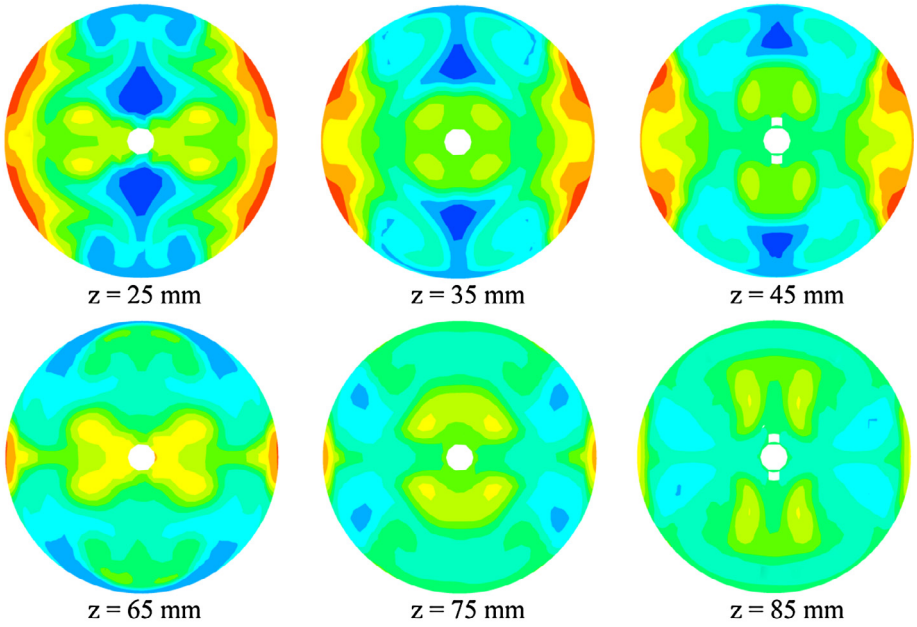

(c)

Fig. 8 (*continued*)

eliminate the inlet effect. The outlet is set as the outflow condition. On the tube wall and surfaces of bidirectional conical strip insert, no slip condition is applied. Radiation and heat conduction of bidirectional conical strip insert are not taken into consideration. The surfaces of bidirectional conical strip insert are regarded as heat insulation surfaces.

$$\text{Inlet velocity profile}: u = u_c\left(1 - \frac{r^2}{R^2}\right) \tag{4}$$

$$\text{Inlet temperature profile}: T = T_c + \frac{qR}{\lambda}\left[\left(\frac{r}{R}\right)^2 - \frac{1}{4}\left(\frac{r}{R}\right)^4\right] \tag{5}$$

where u_c and T_c are the velocity and temperature at the center position of the inlet cross-section, respectively. q is the heat flux imposed on the tube wall. R and r are the inner radius of the tube and the radial distance, respectively.

All the simulations are carried out by using the CFD commercial software Fluent 14.0, based on the finite volume method. The SIMPLE algorithm is applied to achieve the pressure-velocity coupling and second upwind discretization schemes for energy and momentum equations is adopted in numerical simulations. The residuals of less than 10^{-6} for continuity and momentum equations and less than 10^{-8} for energy equation are set as the minimum convergence criterion.

3.2. Computation scheme

The Reynolds number (Re) is defined as:

$$Re = \frac{\rho u_m D}{\mu} \tag{6}$$

where u_m is the mean velocity of fluid in the tube inlet, which is defined as:

$$u_m = \frac{\int_0^R 2\pi r u \, dr}{\int_0^R 2\pi r \, dr} \tag{7}$$

The heat transfer coefficient (h) is written as:

$$h = \frac{q}{T_w - T_m} \tag{8}$$

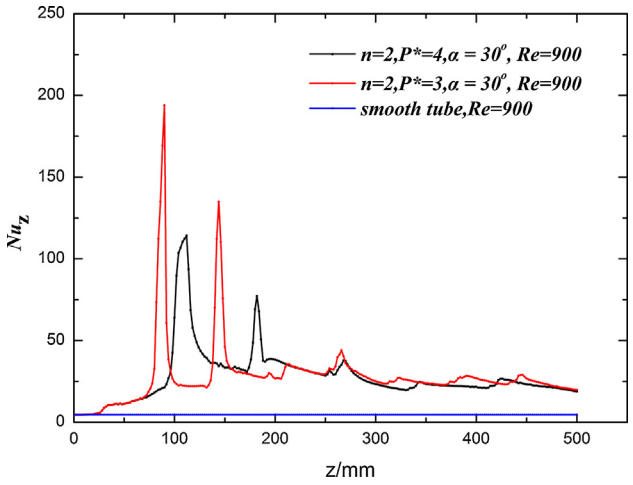

Fig. 9. The local Nusselt number distribution along the flow direction.

where T_w is the average temperature of the tube wall and T_m is fluid bulk temperature inside the tube.

The Nusselt number (Nu) and friction factor (f) are given by:

$$Nu = \frac{hD}{\lambda} \tag{9}$$

$$f = \frac{\Delta P}{\left(\frac{1}{2}\rho u_m^2\right)(L/D)} \tag{10}$$

where ΔP is the difference of the mass-averaged pressure between the inlet and outlet.

To evaluate the overall heat transfer performance of the tube fitted with bidirectional conical strip insert, the widely used performance evaluation criterion (PEC), proposed by Webb [38], is adopted. The formula of PEC is given by:

$$PEC = \frac{Nu/Nu_0}{(f/f_0)^{1/3}} \tag{11}$$

where Nu_0 and f_0 are the average Nusselt number and friction factor of the fully developed smooth tube flow, respectively.

3.3. Grid generation and independence test

The commercial software Gambit 2.4.6 is applied to generate the three-dimensional grid system for computational domain. The grid system consists of hexahedron, pyramid, tetrahedron and prism grids as shown in Fig. 2. Near the tube wall, highly refined prism grids, which are extruded from the surface of the tube wall and perpendicular to the boundary layer, are employed to accurately simulate the boundary layer effects. Near the surfaces of the inserts, local grid refinement is adopted. To improve the quality of the meshes and save computing resources, the majority of the volume is filled with hexahedron grids. Tetrahedron and pyramid grids are generated to fill the gap between the hexahe-

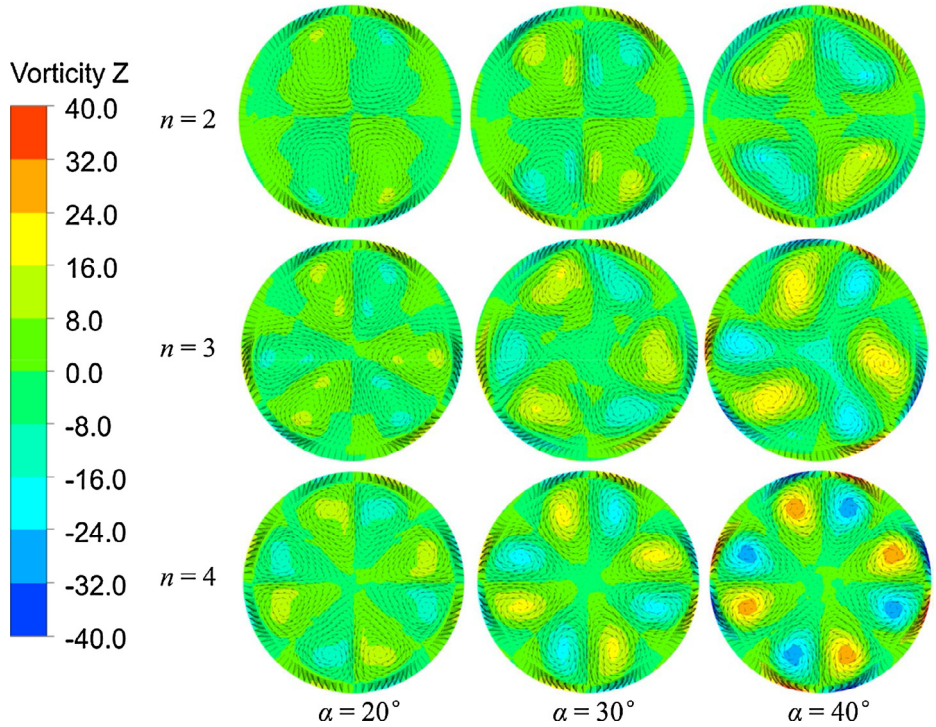

Fig. 10. Tangential velocity vectors and vorticity contours in the z-direction on outlet cross-section of tube with different numbers of bidirectional conical strip and central angles at $P^* = 2$ and $Re = 900$.

dron and prism grids and establish a connection between quadrangle and triangle faces.

Grid independence test is carried out for bidirectional conical strip insert with $n = 2$, $P^* = 2$ and $\alpha = 30°$, at $Re = 900$. Grid systems with four different grid numbers (2,034,253, 4,325,068, 6,252,381 and 8,564,697) are conducted for verifying the accuracy of numerical simulations. From the grid independence test results that displayed in Fig. 3, it is indicated that deviations between the grid systems with 6,252,381 and 8,564,697 elements are sufficiently small, about 1.3% for Nusselt number and 1.1% for friction factor. The grid system with 6,252,381 grid elements is dense enough for the simulations, and thus it is employed in the present work.

4. Validation of numerical model

To validate the accuracy of the numerical methods in simulating characteristics of heat exchange tube with insert, the heat transfer and flow resistance characteristics of tube with curved delta wing vortex generator inserts are simulated by using the numerical methods in this work. And comparison between the numerical results and the experimental results presented in Ref. [26] are shown in Fig. 4. It is clear that the simulation results agree well with the experimental results, and the deviations between numerical and experimental results are limited to 14% for Nusselt number and 12% for friction factor. As the experimental uncertainties are about 14.4% for Nusselt number and 10.3% for friction factor, the deviations between numerical and experimental results, which may be attributed to the unavoidable discrepancies between the numerical methods and experimental measurements, are allowable. Therefore, the numerical model adopted in this study has a reasonable accuracy.

Considering that the flow is expected to depart from the laminar regime toward pulsating or pseudo-laminar flow regime induced by the inserts under the considered Reynolds number range, and to justify that the laminar model applied in the present study is able to wholly capture the flow regime, the inserts with $n = 2$, $P^* = 2$ and $\alpha = 40°$, which induces the strongest disturbance to the fluid, is investigated by using SST k-ω turbulence model [39]. The comparisons of results between the laminar model and SST k-ω turbulence model are displayed in Fig. 5. The deviations between laminar model and SST k-ω turbulence model are limited to 0.9% for Nusselt number and 0.8% for friction factor. Thus, the numerical approach with laminar model is accurate enough to wholly capture the flow regime in the considered Reynolds number range in this study.

5. Results and discussion

5.1. Flow structure and heat transfer

Prior to discussing the heat transfer performance, it is necessary to analyze the flow structures for understanding the mechanism of the heat transfer enhancement in a heat exchange tube fitted with bidirectional conical strip insert. Flow structures in the tube with bidirectional conical strip insert at $Re = 900$, $n = 2$, $P^* = 2$ and $\alpha = 40°$ are shown in Fig. 6. From the Fig. 6(a), it is observed that the fluid in the core region is directed toward the tube wall by the forward conical strips. It is separated at both sides after hitting the tube wall. And then this fluid is replenished to the back of the adjacent reverse conical strips, which can eliminate the possible flow dead zone and eddy on the back of the reverse conical strips and avoid great increase of the pressure loss in the tube flow, as the blue arrows show. Meanwhile, the fluid near the tube wall is directed toward the core region of tube by the reverse conical strips. This fluid is also separated at both sides and replenished to the back of the adjacent forward conical strips, as the red arrows show. The cooperation of the forward and reverse conical strips makes the core fluid and the boundary fluid in the tube rapidly exchanged when the fluid flows through the bidirectional conical strips. Moreover, a longitudinal swirling flow is formed between each pair of adjacent forward and reverse conical strip. Thus, multiple longitudinal swirling flows are generated in tube, as shown in

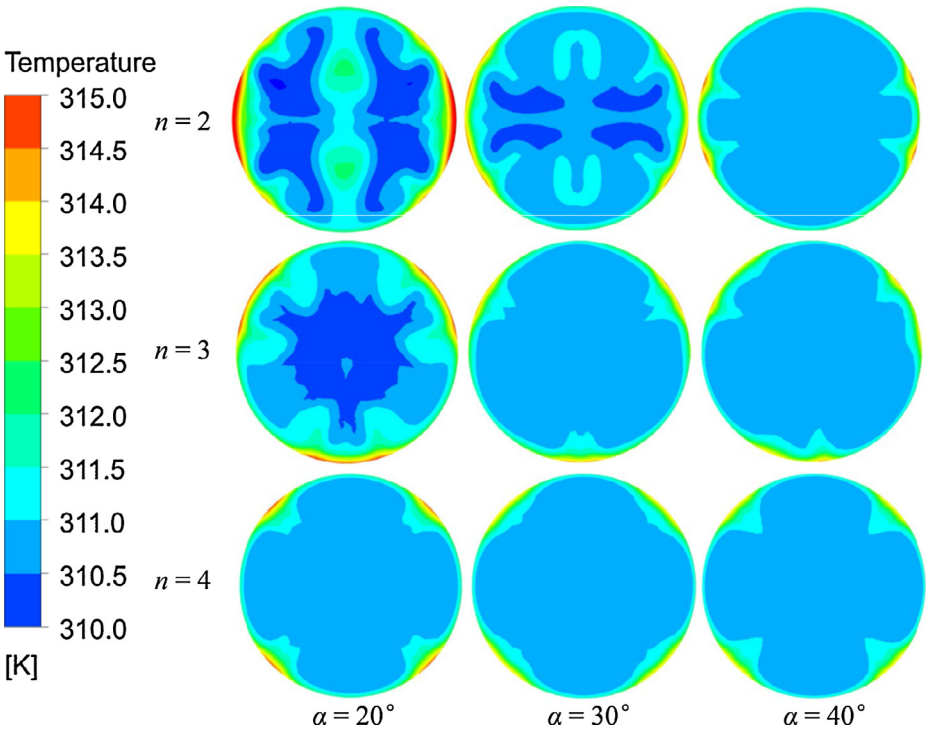

Fig. 11. Temperature contours on outlet cross-section of tube with different numbers of bidirectional conical strip and central angles at $P^* = 2$ and $Re = 900$.

Fig. 6(b). This flow pattern in the tube results in a sufficient flow mixing between cold fluid in core region and hot fluid near the tube wall, and consequently magnifies the temperature gradient of the fluid in thermal boundary layer, hence enhancing the heat transfer.

The circumferential local Nusselt number along the tube wall perimeter is shown in Fig. 7. The circumferential local Nusselt numbers in the areas around 0° and 180°, where withstand a strong fluid impingement induced by the forward conical strips, are greatly enhanced and are much higher than that of the smooth tube, while the circumferential local Nusselt numbers in the areas around 90° and 270°, where the fluid is guided back to the core region by the reverse conical strips, are apparently lower than that in the areas around 0° and 180° but higher than that of the smooth tube. In general, the average Nusselt numbers of the enhanced tubes are effectively improved compared to smooth tube.

Fig. 8(a) and (b) show the tangential velocity vectors and temperature distributions in axial sections of tube with bidirectional conical strip insert at $Re = 900$, $n = 2$, $P^* = 2$ and $\alpha = 40°$. It is clear that the fluid is guided to the tube wall by forward conical strips, and the fluid on back of forward conical strips is also drawn to the tube wall. Therefore, the cold fluid in the core region is drawn to the boundary of the tube wall. Similarly, the hot fluid near the tube wall is guided and drawn to the core region of the tube by reverse conical strips. Fig. 8(c) shows the temperature contours of different cross sections. It is observed that the hot fluid at the boundary and the cold fluid in core region are rapidly exchanged and sufficiently mixed when the fluid flows through the bidirectional conical strips. The temperature of the fluid near the wall is significantly reduced and the temperature gradient near the tube wall is effectively increased. As a result, the heat transfer performance is remarkably improved.

The local Nusselt number distributions along the flow direction of enhanced tubes and smooth tube are shown in Fig. 9. It is clear that the local Nusselt number along the flow direction of smooth tube is always around 4.36, which is the theoretical value of the fully developed tube flow. For enhanced tube, the local Nusselt number fluctuates significantly in the first two periods, and then tends to be stable. It is because that the hot fluid near the tube wall and the cold fluid in core region are rapidly exchanged in the first two periods, and then the temperature of the fluid tends to be uniform. In addition, the local Nusselt numbers of enhanced tubes are much higher than that of the smooth tube, which means the heat transfer performance of the enhanced tube, compared to the smooth tube, is remarkably improved.

5.2. Effects of geometric parameters

Fig. 10 shows the tangential velocity vectors and vorticity contours in the z-direction on outlet cross-section of tube fitted with

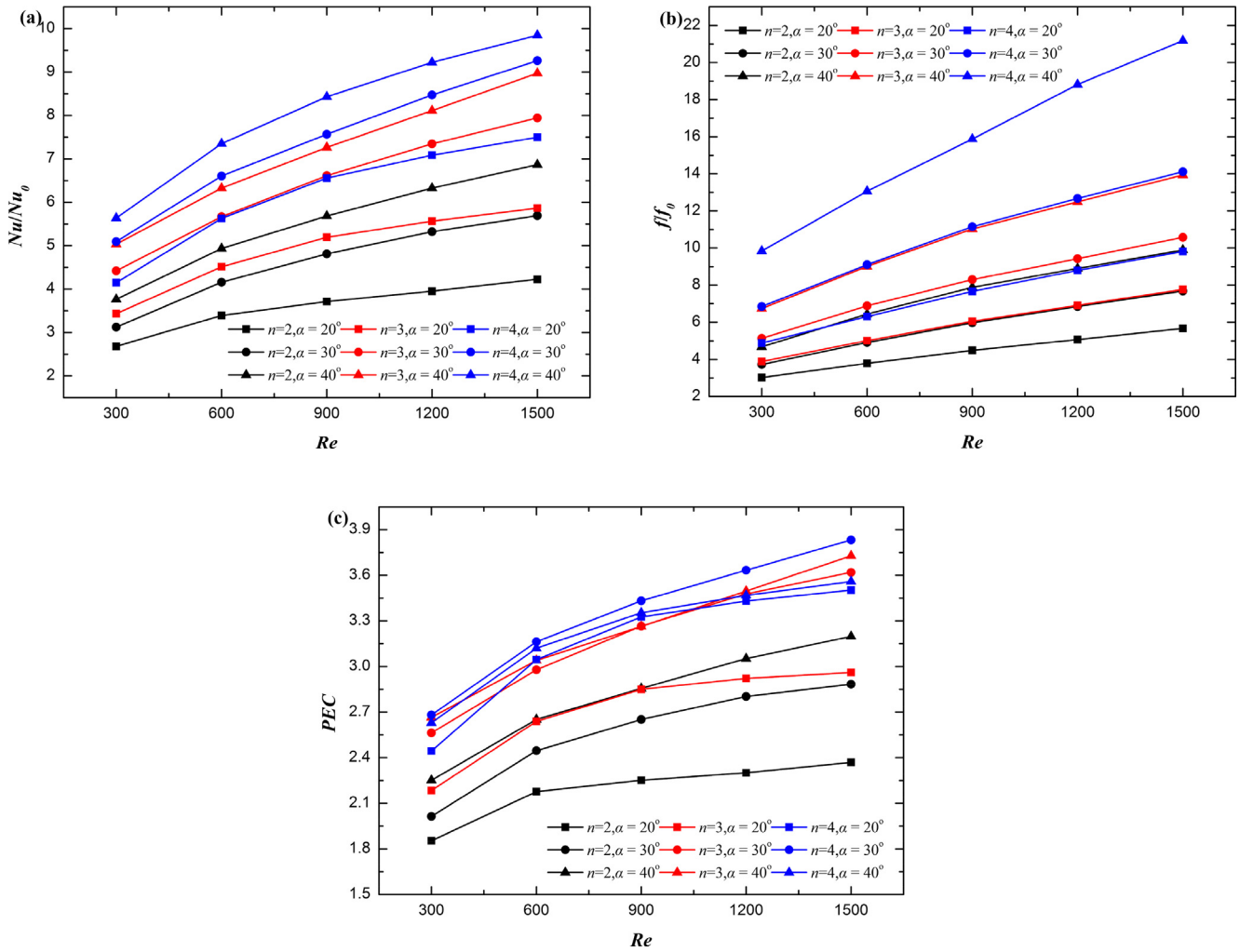

Fig. 12. Effects of the number of bidirectional conical strip and central angle on the heat transfer, flow resistance and overall thermal performance at $P^* = 2$: (a) Nusselt number ratio; (b) friction factor ratio; (c) *PEC* values.

inserts with different numbers of bidirectional conical strip and central angles at $P^* = 2$ and $Re = 900$. It is clear that two, three and four pairs of multiple longitudinal swirl flows are generated in the tube with bidirectional conical strip insert for $n = 2$, 3 and 4, respectively. Moreover, the vorticity in z-direction increases with the increase of the number of bidirectional conical strip and central angle, which means that the disturbance to the fluid is greater and the mixing of the fluid is more sufficient at a larger number of bidirectional conical strip or a larger central angle.

The temperature contours on outlet cross-section of tube fitted with inserts with different numbers of bidirectional conical strip and central angles at $P^* = 2$ and $Re = 900$ is displayed Fig. 11. It is obvious that the temperature distribution of the outlet cross-section becomes more uniform as the number of bidirectional conical strip and central angle increase. Moreover, the temperature gradient near the tube wall increases with the increase of the number of bidirectional conical strip and central angle. Therefore, the heat transfer coefficient in the tube increases with the increasing number of bidirectional conical strip and central angle.

Fig. 12 shows the variations of the Nusselt number ratio, friction factor ratio and the overall heat transfer performance (*PEC*) with the numbers of bidirectional conical strip and central angles at $P^* = 2$. The effect of the number of bidirectional conical strip is described by lines of the same symbols and different colors, while the effect of the central angle is described by the lines of the same colors and different symbols. Based on the analysis of Figs. 10 and 11 above, it is easy to understand that both the Nusselt number ratio and friction factor ratio increase with the increase of the numbers of bidirectional conical strip and central angles. From Fig. 12(b), we found a phenomenon that when $n \times \alpha$ is the same, the friction factor ratio is basically coincident. It may be because when $n \times \alpha$ is the same, the area of conical strips that facing the flow is the same, and the viscous dispassion and kinetic energy losses caused by the inserts may be the same. Therefore, the flow resistance is consequently coincident. In addition, under the larger number of bidirectional conical strip, the friction factor ratio increases faster along with the increase of the central angle. Therefore, when $n = 2$, the *PEC* value increase with the increasing central angle; when $n = 3$, the *PEC* values of $\alpha = 30°$ and 40° are roughly the same and larger than that of $\alpha = 20°$; when $n = 4$, the moderate central angle $\alpha = 30°$ can obtain the largest *PEC* value, as shown in Fig. 12(c).

To analyze the effect of the pitch ratio, results of outlet cross-section of tube with different pitch ratios at $Re = 900$, $n = 3$, and $\alpha = 30°$ are displayed in Fig. 13. As the pitch ratio decreases, the vorticity contours in the z-direction gets stronger, which means the disturbance to the fluid increases. And the temperature distribution of the outlet cross-section becomes more uniform with the decreasing pitch ratio. The stronger disturbance to the fluid and more uniform of temperature distribution result in larger flow resistance and higher heat transfer coefficient, respectively. Thus, both the Nusselt number ratio and the friction factor ratio increase with the decreasing pitch ratio, as shown in Fig. 14(a) and (b). But the friction factor is more sensitive to the pitch ratio. Therefore, the *PEC* value increases with the increase of pitch ratio, as shown in Fig. 14(c).

5.3. Correlations for Nusselt number and friction factor

In order to predict the heat transfer and flow resistance, correlations for Nusselt number and friction factor are derived from the cases with three pitch ratios, three numbers of bidirectional conical strip, three central angles and five Reynolds numbers. The formulas of correlations are given as follows:

$$Nu = 0.24781 Re^{0.33946} n^{0.56548} P^{*-0.1595} \alpha^{0.55242} \quad (12)$$

$$f = 1.2373 Re^{-0.54603} n^{0.81067} P^{*-0.53792} \alpha^{0.75412} \quad (13)$$

where the ranges of the parameters in this study are that $Re = 300$–1500, $n = 2$–4, $P^* = 2.0$–4.0, $\alpha = 20°$–40°.

The Nusselt numbers and friction factors predicted from Eqs. (12) and (13) agree well with the numerical results with the devi-

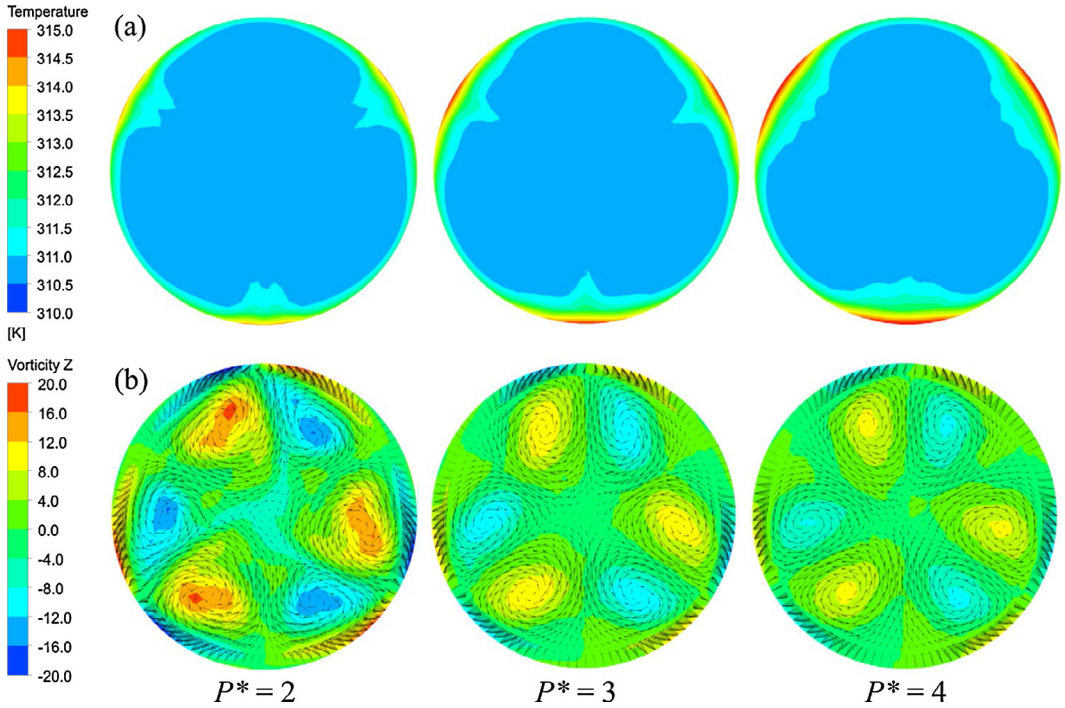

Fig. 13. Results of outlet cross-section of tube with different pitch ratios at $Re = 900$, $n = 3$, and $\alpha = 30°$, (a) temperature contours; (b) tangential velocity vectors and vorticity contours in the z-direction.

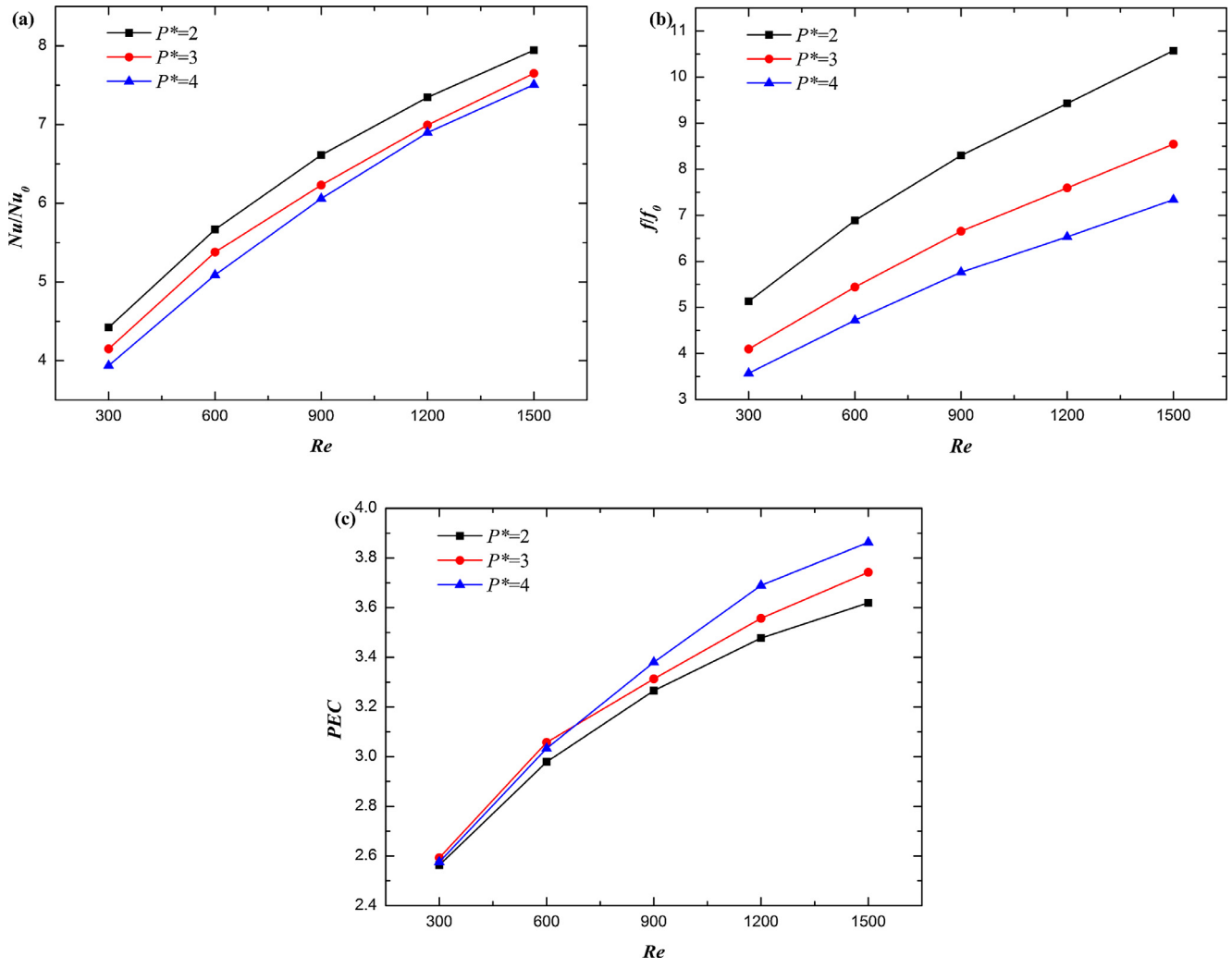

Fig. 14. Effects of pitch ratio on the heat transfer and flow performance at $n = 3$, $\alpha = 30°$: (a) Nusselt number ratio; (b) friction factor ratio; (c) *PEC* values.

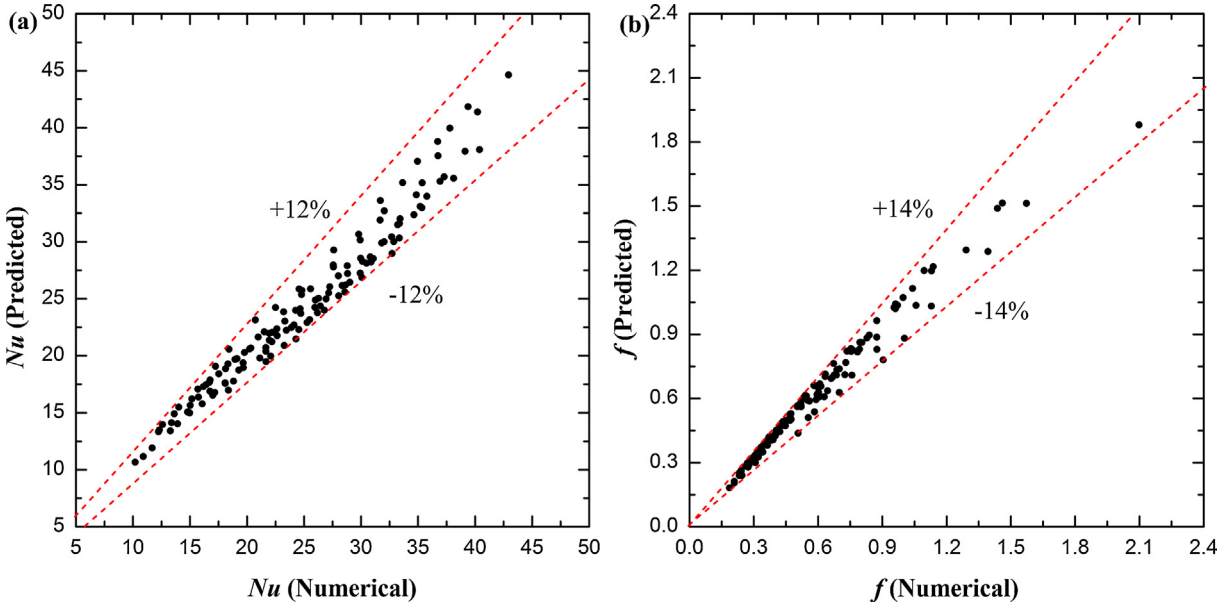

Fig. 15. Comparisons of Nusselt number and friction factor between correlations and numerical results: (a) Nusselt number, (b) friction factor.

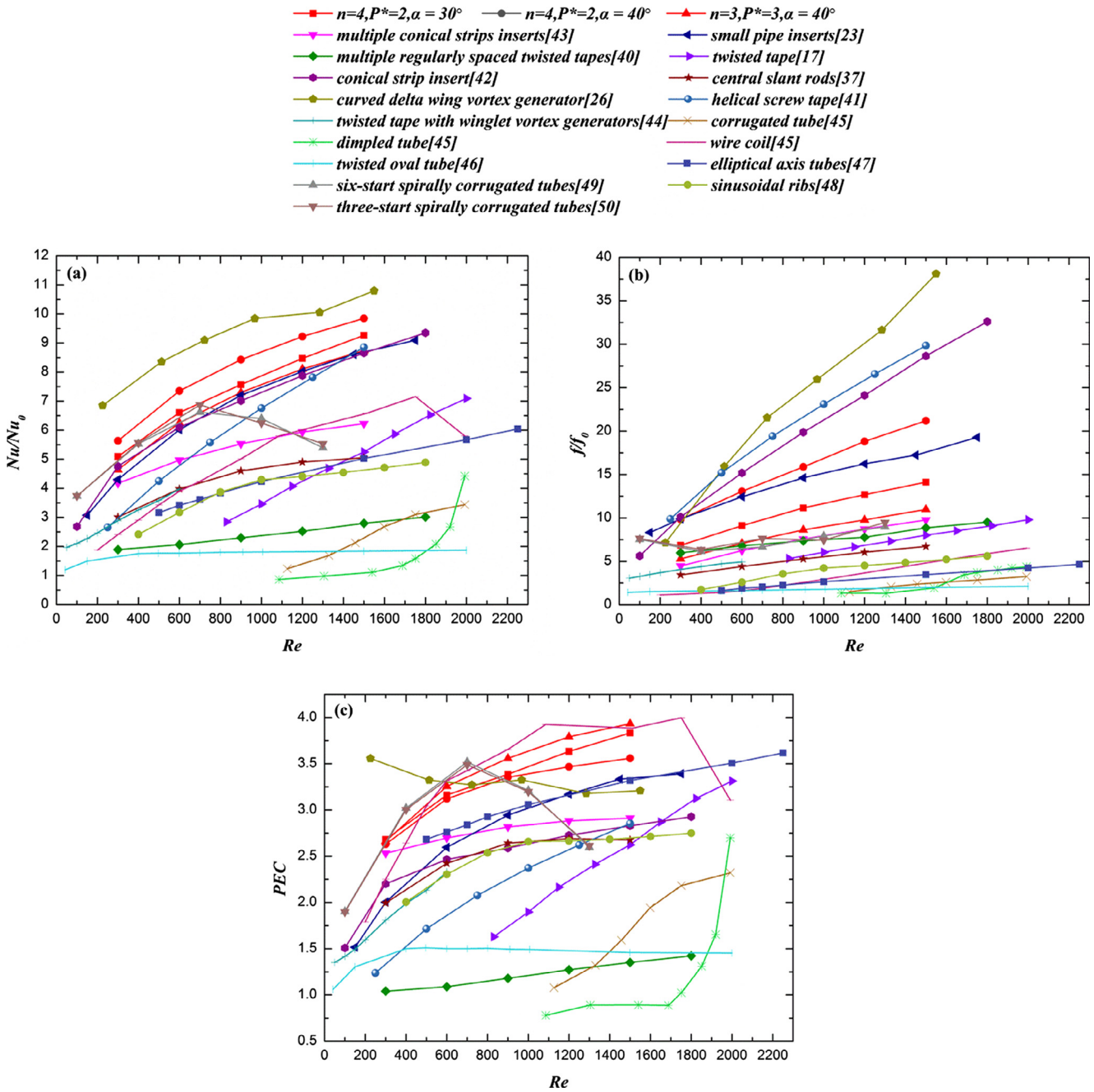

Fig. 16. Comparisons between the present work and previous works (a) Nusselt number ratio, (b) friction factor ratio, (c) *PEC* value.

ations limited to ±12% for Nusselt number and ±14% for friction factor, as shown in Fig. 15.

5.4. Comparison with previous works

The comparisons of Nusselt number ratio, friction factor ratio and overall heat transfer performance (*PEC*) with the previous works, including multiple regularly spaced twisted tapes [40], twisted tape [17], helical screw tape [41],small pipe inserts [23], conical strip insert [42], multiple conical strip inserts [43], curved delta wing vortex generator [26], central slant rod [37], twisted tape with winglet vortex generators [44] and several corrugated tubes [45–50], are shown in Fig. 16(a)–(c). It is clear that the heat transfer of the bidirectional conical strip inserts is lower than that of the curved delta wing vortex generator. However, the pressure drop in the present work is much lower than that of the curved delta wing vortex generator. Hence, the overall heat transfer performance of the bidirectional conical strip inserts is higher than that of the curved delta wing vortex generator at a higher Reynolds number. Compared to other previous works in Fig. 16, the bidirectional conical strip inserts obtains a higher heat transfer coefficient but a moderate flow resistance, and therefore achieves a higher overall heat transfer performance.

6. Conclusions

In this paper, a novel tube insert (bidirectional conical strip inserts) is proposed for heat transfer enhancement, and the heat transfer performance and flow characteristics of this insert are

studied numerically. The flow structure and mechanism of heat transfer performance are analyzed. Moreover, the effects of three geometric parameters (numbers of bidirectional conical strip, central angle and pitch ratio) are also investigated. The following conclusions are obtained.

(1) As the fluid flows through the bidirectional conical strip, the cold fluid in the core region is rapidly exchanged with the hot fluid near the tube wall. And multiple longitudinal swirling flows are formed downstream of the bidirectional conical strip, which result in a sufficient flow mixing and a larger temperature gradient of the fluid in thermal boundary layer, thereby enhance the heat transfer. Moreover, the combination of the forward and reverse conical strips inhibits or eliminates the formation of the dead zone and eddy on the back of the conical strips. Therefore, the increase in flow resistance is relative smaller than relevant published works. The average Nusselt number and friction factor of tube with bidirectional conical strip inserts are 2.35–9.85 and 2.37–21.18 times those of smooth tube, respectively. The PEC values in tube with bidirectional conical strip inserts vary from 1.75 to 3.93.
(2) Both the Nusselt number and friction factor increase with the increase of numbers of bidirectional conical strip, central angle and the decrease of pitch ratio. And the maximum overall heat transfer performance (*PEC* value) was obtained by geometric model with $n = 3$, $\alpha = 40^\circ$ and $P^* = 3$.
(3) Correlation formulas are derived with the deviations limited to ±12% for Nusselt number and ±14% for friction factor.
(4) Compared to the relevant published works, the bidirectional conical strip inserts can obtain a higher heat transfer without much increase in flow resistance, and therefore achieve a high overall heat transfer performance.

Conflict of interest

Authors declared that there is no conflict of interest.

Acknowledgments

The work was supported by the National Natural Science Foundation of China (Grant No. 51736004), the National Natural Science Foundation of China (51376069) and the National Natural Science Foundation of China Youth Project (51606073).

Appendix A. Supplementary material

Supplementary data associated with this article can be found, in the online version, at https://doi.org/10.1016/j.ijheatmasstransfer.2018.07.128.

References

[1] M. Sheikholeslami, M. Gorji-Bandpy, D.D. Ganji, Review of heat transfer enhancement methods: focus on passive methods using swirl flow devices, Renew. Sustain. Energy Rev. 49 (2015) 444–469.
[2] S. Liu, M. Sakr, A comprehensive review on passive heat transfer enhancements in pipe exchangers, Renew. Sustain. Energy Rev. 19 (2013) 64–81.
[3] W. Fuqiang, L. Qingzhi, H. Huaizhi, T. Jianyu, Parabolic trough receiver with corrugated tube for improving heat transfer and thermal deformation characteristics, Appl. Energy 164 (2016) 411–424.
[4] Z.-J. Jin, F.-Q. Chen, Z.-X. Gao, X.-F. Gao, J.-Y. Qian, Effects of pitch and corrugation depth on heat transfer characteristics in six-start spirally corrugated tube, Int. J. Heat Mass Transf. 108 (2017) 1011–1025.
[5] W. Wang, Y. Zhang, B. Li, H. Han, X. Gao, Influence of geometrical parameters on turbulent flow and heat transfer characteristics in outward helically corrugated tubes, Energy Convers. Manage. 136 (2017) 294–306.
[6] Z.S. Kareem, M.N. Mohd Jaafar, T.M. Lazim, S. Abdullah, A.F. Abdulwahid, Passive heat transfer enhancement review in corrugation, Exp. Therm Fluid Sci. 68 (2015) 22–38.
[7] W. Xu, S. Wang, Q. Zhang, Q. Wang, H. Lu, H. Tan, Experimental and numerical studies of heat transfer and friction factor of therminol liquid phase heat transfer fluid in a ribbed tube, Appl. Therm. Eng. 95 (2016) 165–177.
[8] W. Xu, S. Wang, G. Liu, Q. Zhang, M. Hassan, H. Lu, Experimental and numerical investigation on heat transfer of Therminol heat transfer fluid in an internally four-head ribbed tube, Int. J. Therm. Sci. 116 (2017) 32–44.
[9] K. Bilen, M. Cetin, H. Gul, T. Balta, The investigation of groove geometry effect on heat transfer for internally grooved tubes, Appl. Therm. Eng. 29 (4) (2009) 753–761.
[10] Y.S. Chen, J. Tian, Y. Fu, Z.F. Tang, H.H. Zhu, N.X. Wang, Experimental study of heat transfer enhancement for molten salt with transversely grooved tube heat exchanger in laminar-transition-turbulent regimes, Appl. Therm. Eng. 132 (2018) 95–101.
[11] Y.-H. Wang, J.-L. Zhang, Z.-X. Ma, Experimental determination of single-phase pressure drop and heat transfer in a horizontal internal helically-finned tube, Int. J. Heat Mass Transf. 104 (2017) 240–246.
[12] A.R. Sajadi, S. Yamani Douzi Sorkhabi, D. Ashtiani, F. Kowsari, Experimental and numerical study on heat transfer and flow resistance of oil flow in alternating elliptical axis tubes, Int. J. Heat Mass Transf. 77 (2014) 124–130.
[13] R. Manglik, A. Bergles, Heat transfer and pressure drop correlations for twisted-tape inserts in isothermal tubes: part I–laminar flows, Trans.-Am. Soc. Mech. Eng. J. Heat Transf. 115 (1993), 881 881.
[14] R.M. Manglik, A.E. Bergles, Heat transfer and pressure drop correlations for twisted-tape inserts in isothermal tubes: Part II—Transition and turbulent flows, J. Heat Transf. 115 (4) (1993) 890–896.
[15] Varun, M.O. Garg, H. Nautiyal, S. Khurana, M.K. Shukla, Heat transfer augmentation using twisted tape inserts: a review, Renew. Sustain. Energy Rev. 63 (2016) 193–225.
[16] S.K. Saha, A. Dutta, S.K. Dhal, Friction and heat transfer characteristics of laminar swirl flow through a circular tube fitted with regularly spaced twisted-tape elements, Int. J. Heat Mass Transf. 44 (22) (2001) 4211–4223.
[17] K. Wongcharee, S. Eiamsa-Ard, Friction and heat transfer characteristics of laminar swirl flow through the round tubes inserted with alternate clockwise and counter-clockwise twisted-tapes, Int. Commun. Heat Mass Transf. 38 (3) (2011) 348–352.
[18] J. Guo, A. Fan, X. Zhang, W. Liu, A numerical study on heat transfer and friction factor characteristics of laminar flow in a circular tube fitted with center-cleared twisted tape, Int. J. Therm. Sci. 50 (7) (2011) 1263–1270.
[19] P. Murugesan, K. Mayilsamy, S. Suresh, P. Srinivasan, Heat transfer and pressure drop characteristics in a circular tube fitted with and without V-cut twisted tape insert, Int. Commun. Heat Mass Transf. 38 (3) (2011) 329–334.
[20] A. Saysroy, S. Eiamsa-ard, Periodically fully-developed heat and fluid flow behaviors in a turbulent tube flow with square-cut twisted tape inserts, Appl. Therm. Eng. 112 (2017) 895–910.
[21] A.R.S. Suri, A. Kumar, R. Maithani, Heat transfer enhancement of heat exchanger tube with multiple square perforated twisted tape inserts: Experimental investigation and correlation development, Chem. Eng. Process. Process Intensif. 116 (2017) 76–96.
[22] V. Ozceyhan, S. Gunes, O. Buyukalaca, N. Altuntop, Heat transfer enhancement in a tube using circular cross sectional rings separated from wall, Appl. Energy 85 (10) (2008) 988–1001.
[23] W. Tu, Y. Tang, J. Hu, Q. Wang, L. Lu, Heat transfer and friction characteristics of laminar flow through a circular tube with small pipe inserts, Int. J. Therm. Sci. 96 (2015) 94–101.
[24] A. Fan, J. Deng, A. Nakayama, W. Liu, Parametric study on turbulent heat transfer and flow characteristics in a circular tube fitted with louvered strip inserts, Int. J. Heat Mass Transf. 55 (19) (2012) 5205–5213.
[25] C. Zhang, D. Wang, Y. Zhu, Y. Han, J. Wu, X. Peng, Numerical study on heat transfer and flow characteristics of a tube fitted with double spiral spring, Int. J. Therm. Sci. 94 (2015) 18–27.
[26] P.W. Deshmukh, S.V. Prabhu, R.P. Vedula, Heat transfer enhancement for laminar flow in tubes using curved delta wing vortex generator inserts, Appl. Therm. Eng. 106 (2016) 1415–1426.
[27] M. Pourramezan, H. Ajam, Modeling for thermal augmentation of turbulent flow in a circular tube fitted with twisted conical strip inserts, Appl. Therm. Eng. 105 (2016) 509–518.
[28] X.W. Zhu, Y.H. Fu, J.Q. Zhao, A novel wavy-tape insert configuration for pipe heat transfer augmentation, Energy Convers. Manage. 127 (2016) 140–148.
[29] P.B. Jasiński, Numerical study of thermo-hydraulic characteristics in a circular tube with ball turbulators. Part 3: Thermal performance analysis, Int. J. Heat Mass Transf. 107 (2017) 1138–1147.
[30] K. Nanan, C. Thianpong, M. Pimsarn, V. Chuwattanakul, S. Eiamsa-ard, Flow and thermal mechanisms in a heat exchanger tube inserted with twisted cross-baffle turbulators, Appl. Therm. Eng. 114 (2017) 130–147.
[31] Z. Cao, J. Xu, D. Sun, J. Xie, F. Xing, Q. Chen, X. Wang, Numerical simulation of modulated heat transfer tube in laminar flow regime, Int. J. Therm. Sci. 75 (2014) 171–183.
[32] Z. Cao, J. Xu, Modulated heat transfer tube with short conical-mesh inserts: a linking from microflow to macroflow, Int. J. Heat Mass Transf. 89 (2015) 291–307.
[33] J.-A. Meng, X.-G. Liang, Z.-X. Li, Field synergy optimization and enhanced heat transfer by multi-longitudinal vortexes flow in tube, Int. J. Heat Mass Transf. 48 (16) (2005) 3331–3337.

[34] W. Liu, Z. Liu, H. Jia, A. Fan, A. Nakayama, Entransy expression of the second law of thermodynamics and its application to optimization in heat transfer process, Int. J. Heat Mass Transf. 54 (13) (2011) 3049–3059.
[35] H. Jia, Z.C. Liu, W. Liu, A. Nakayama, Convective heat transfer optimization based on minimum entransy dissipation in the circular tube, Int. J. Heat Mass Transf. 73 (2014) 124–129.
[36] W. Liu, P. Liu, J.B. Wang, N.B. Zheng, Z.C. Liu, Exergy destruction minimization: a principle to convective heat transfer enhancement, Int. J. Heat Mass Transf. 122 (2018) 11–21.
[37] P. Liu, N. Zheng, F. Shan, Z. Liu, W. Liu, Numerical study on characteristics of heat transfer and friction factor in a circular tube with central slant rods, Int. J. Heat Mass Transf. 99 (2016) 268–282.
[38] R. Webb, Performance evaluation criteria for use of enhanced heat transfer surfaces in heat exchanger design, Int. J. Heat Mass Transf. 24 (4) (1981) 715–726.
[39] M.K.F. Menter, R. Langtry, Ten years of industrial experience with the SST turbulence model, Turbulence, Heat Mass Transf. 4 (2003).
[40] X. Zhang, Z. Liu, W. Liu, Numerical studies on heat transfer and flow characteristics for laminar flow in a tube with multiple regularly spaced twisted tapes, Int. J. Therm. Sci. 58 (2012) 157–167.
[41] P. Sivashanmugam, S. Suresh, Experimental studies on heat transfer and friction factor characteristics of laminar flow through a circular tube fitted with helical screw-tape inserts, Appl. Therm. Eng. 26 (16) (2006) 1990–1997.
[42] Y. You, A. Fan, W. Liu, S. Huang, Thermo-hydraulic characteristics of laminar flow in an enhanced tube with conical strip inserts, Int. J. Therm. Sci. 61 (2012) 28–37.
[43] P. Liu, N. Zheng, F. Shan, Z. Liu, W. Liu, An experimental and numerical study on the laminar heat transfer and flow characteristics of a circular tube fitted with multiple conical strips inserts, Int. J. Heat Mass Transf. 117 (Supplement C) (2018) 691–709.
[44] Z.-M. Lin, L.-B. Wang, M. Lin, W. Dang, Y.-H. Zhang, Numerical study of the laminar flow and heat transfer characteristics in a tube inserting a twisted tape having parallelogram winglet vortex generators, Appl. Therm. Eng. 115 (2017) 644–658.
[45] A. García, J.P. Solano, P.G. Vicente, A. Viedma, The influence of artificial roughness shape on heat transfer enhancement: corrugated tubes, dimpled tubes and wire coils, Appl. Therm. Eng. 35 (2012) 196–201.
[46] J. Cheng, Z. Qian, Q. Wang, Analysis of heat transfer and flow resistance of twisted oval tube in low Reynolds number flow, Int. J. Heat Mass Transf. 109 (2017) 761–777.
[47] J.-A. Meng, X.-G. Liang, Z.-J. Chen, Z.-X. Li, Experimental study on convective heat transfer in alternating elliptical axis tubes, Exp. Therm Fluid Sci. 29 (4) (2005) 457–465.
[48] J. Du, Y. Hong, S.-M. Huang, W.-B. Ye, S. Wang, Laminar thermal and fluid flow characteristics in tubes with sinusoidal ribs, Int. J. Heat Mass Transf. 120 (2018) 635–651.
[49] H.H. Balla, Enhancement of heat transfer in six-start spirally corrugated tubes, Case Stud. Therm. Eng. 9 (2017) 79–89.
[50] Z.S. Kareem, S. Abdullah, T.M. Lazim, M.N. Mohd Jaafar, A.F. Abdul Wahid, Heat transfer enhancement in three-start spirally corrugated tube: Experimental and numerical study, Chem. Eng. Sci. 134 (2015) 746–757.